Vapor–Liquid Equilibrium in the Binary System Carbon Dioxide + *n*-Butane

Maria E. Pozo de Fernández,[†] **John A. Zollweg,* and William B. Streett**

School of Chemical Engineering, Olin Hall, Cornell University, Ithaca, New York 14853

Vapor–liquid equilibrium measurements (P–T–x–y) have been performed on mixtures of carbon dioxide/*n*-butane (CO_2/*n*-C_4), at nine temperatures from 4.75 °C (277.90 K) to 145.33 °C (418.48 K) and at pressures up to 8.17 MPa (1185 psia). Two isotherms lie below the critical temperature of CO_2 (31.04 °C, 304.19 K), where both components are subcritical, and seven were measured between the CO_2 and *n*-C_4 critical temperatures, up to the mixture critical line. The data have been obtained with a vapor-recirculating apparatus working at isothermal conditions. A liquid bath was used for isotherms below 80 °C, and an oven was used for the high-temperature isotherms. The results obtained were in good agreement with previous measurements done for the system. The data were also correlated by using two cubic equations of state, the Soave–Redlich–Kwong and the Peng–Robinson equations.

Introduction

This study of vapor–liquid equilibrium is the fifth in a series involving CO_2 as one component and a hydrocarbon as the other one. The previous systems were CO_2/*n*-pentane (*1*), CO_2/isopentane (*2*), CO_2/neopentane (*3*), and CO_2/cyclopentane (*4*). All the measurements in the reported systems have been taken up to the critical locus of the mixtures.

These experimental values should be useful for the gas and petroleum industry for a better understanding of tertiary oil recovery methods, where knowledge of the phase equilibrium behavior plays an important role in the design of the separation process. Others have made isothermal measurements in different regions of the phase diagram (*5–9*), but their work was limited to high (*5*), medium (*6*, *7*), or low temperatures (*8*, *9*). This is the most comprehensive study of the system over a wide range of temperatures, up to the mixture critical line.

This paper presents the tabulated experimental (P–T–x–y) data for nine isotherms, from 277.9 to 418.48 K and the results obtained by correlating the data to the Soave–Redlich–Kwong and the Peng–Robinson equations of state.

Experimental Section

A vapor-recirculating equilibrium system was used, and measurements of the compositions of coexisting liquid and vapor phases were made as a function of pressure at selected fixed temperatures. The apparatus and methods used in this work were similar to those used in earlier studies (*4*, *10*).

Two sets of apparatus were used depending on the isotherm under study. For the low-temperature isotherms ($T < 80$ °C), a liquid bath was used, having a mixture of water and commercial antifreeze as bath fluid. The temperature of the bath was regulated by a proportional controller. The high-temperature isotherms ($T > 80$ °C) were studied in a commercial windowed oven. The temperature was measured in either case by a platinum resistance thermometer, calibrated according to IPTS-68 accurate to ± 0.02 °C. Both apparatuses had an equilibrium cell made of synthetic sapphire, which provided visibility of the mixture over the entire pressure and temperature range covered in this work. The pressure was measured by use of a digital pressure gauge (Autoclave Eng., Inc. Model DPS-0021) calibrated against a direct-reading Ruska quartz spiral gauge.

The mixture was analyzed by using a gas chromatograph (Hewlett-Packard 5840A) employing a thermal conductivity detector. A stainless steel column, 0.3125 cm ($^1/_8$ in.) o.d. and 50.8 cm (20 in.) long, packed with Porapak Q, 100/120 mesh, was used as the separating medium. The column gave a good resolution of the binary mixture over the entire range of compositions. Two columns were used, one for analysis, and the other as a reference, to reduce base-line drift in the chromatograms.

The operating temperature of the chromatograph oven was set initially at 80 °C. After the emergence of the first peak, corresponding to CO_2 (retention times between 0.19 and 0.27 min), the oven temperature was increased at 28 °C/min, starting 0.5 min after the beginning of the run. This served to accelerate the passage of *n*-butane through the column (retention times between 2.0 and 2.4 min), reaching a final temperature of 150 °C. The runs lasted an average of 4–5 min. The temperature at the thermal conductivity detector was set at 200 °C. The temperature of the auxiliary valve and injection port was 130 °C. Helium was used as the carrier gas in both columns, at a rate of 25 mL/min.

A calibration curve was obtained to translate the area percentage values given by the chromatograms to the true mole fractions of the components in the mixtures. Calibration mixtures were prepared by gravimetry. The errors in the mass measurements while preparing these mixtures were estimated at ±0.0002 g. The values of the chromatogram area fraction for CO_2 ($A_1\%$) were plotted against the CO_2 mole fractions. Also, a plot of $(y - A\,\%)_1$ vs $A_1\%$ was made, in order to observe the scattering in the data. A third degree polynomial curve was fit to the experimental points by the method of least squares.

$$y_1 = 1.56841(A_1\%) - 0.713056(A_1\%)^2 + 0.144642(A_1\%)^3 \quad (1)$$

where y_1 = CO_2 mole fraction and $A_1\%$ = CO_2 area precentage reported on the chromatogram. By use of this equation, mole fraction values could be obtained with any $A_1\%$ value reported on the chromatogram.

Chemicals

The carbon dioxide used in this work was supplied by Air Products and Chemicals, Inc., shipped as a liquefied gas under its own vapor pressure, with a stated purity of 99.99%. The *n*-butane was supplied by Phillips Petroleum Co., shipped as a liquefied gas under its own vapor pressure, with a stated purity of 99.99 mol%. Both components were used without further purification.

---

* Author to whom correspondence should be addressed.

[†] Present address: Departamento de Termodinámica y Fenómenos de Transferencia, Universidad Simón Bolivar, Caracas 1086-A, Venezuela.

0021-9568/89/1734-0324$01.50/0

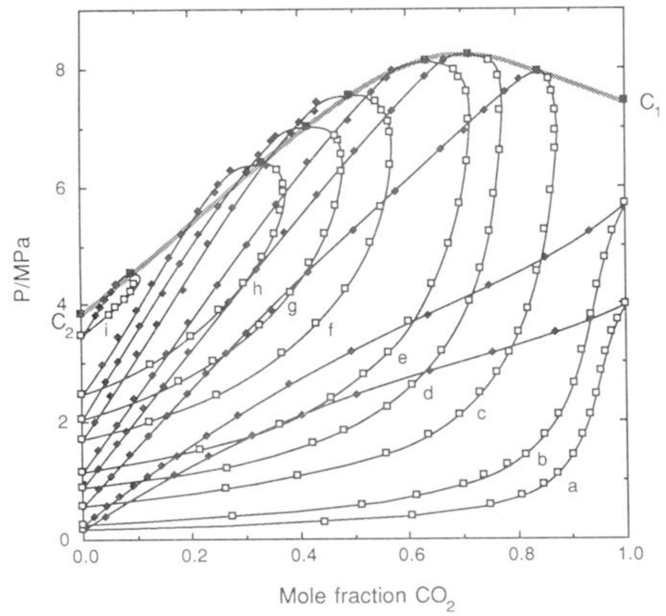

Figure 1. Pressure–composition diagram. The gray curve is the mixture critical line extending from the critical point of CO_2 (C_1) to the critical point of *n*-butane (C_2). Liquid mole fractions (*x*) are shown by ● and vapor mole fractions (*y*) by □. Isotherms are labeled (a) 277.60, (b) 292.60, (c) 325.01, (d) 344.25, (e) 357.77, (f) 377.55, (g) 387.62, (h) 397.89, and (i) 418.48 K.

Results

Vapor–liquid equilibrium measurements for nine isotherms have been obtained in the temperature range from 4.75 to 145.33 °C (277.90–418.48 K) and at pressures up to 8.17 MPa (1185 psia).

The experimental data points are presented in Table I. The reported values for the mixture critical line are summarized in Table II. To facilitate the data display, the following notation was used throughout the tables: T = temperature (K); P = pressure (MPa); x_1 = mole fraction of component 1 (CO_2) in the liquid phase; y_1 = mole fraction of component 1 (CO_2) in the vapor phase. Uncertainties in the phase compositions are estimated to be ±0.005, except in the critical region, where the uncertainties could be as high as ±0.01.

The results obtained have been plotted in a pressure–composition (P–x–y) diagram, shown in Figure 1. The isotherms have a broad coexistence region between the liquid and the vapor phases, showing also a small positive deviation from Raoult's law. This type of behavior had been observed in other CO_2–paraffin hydrocarbon systems, from C_3 to C_{12} (*13*).

Each isotherm obtained above the critical temperature of CO_2 (T_c = 31.04 °C) ended at a mixture critical point, shown as a square on the isotherms in Figure 1. When the mixture was approaching the critical point, it was quite difficult to distinguish between the vapor and the liquid phases, since the meniscus was becoming very diffuse. The critical point was approached by adding small quantities of either component, to avoid upsetting the delicate balance of phase volumes.

Very near the critical line, critical opalescence was observed. A "cloud" was formed at the bottom of the cell, gradually covering the whole cell. The cloud appeared blue in reflected light and brown in transmitted light. When the pressure was increased just above the critical value, the cloud disappeared and only one phase was observed.

The projection of the mixture critical line on the P–x plane is continuous between the critical points of the pure components, showing a maximum in pressure at a temperature close to 71 °C. The measured mixture critical line is reported in Table II and plotted on a pressure–temperature (P–T) diagram in Figure 2. The vapor–liquid coexistence region is bounded by three lines: the vapor pressure curve of pure carbon dioxide (A–C_1), the vapor pressure curve of pure *n*-butane (B–C_2), and the mixture critical line (C_1–C_2). The pressure–temperature domain covered in this study is shown by the shaded area in Figure 2. The system CO_2/*n*-butane belongs to class I, following the classification scheme suggested by van Konynenburg and Scott (*14*).

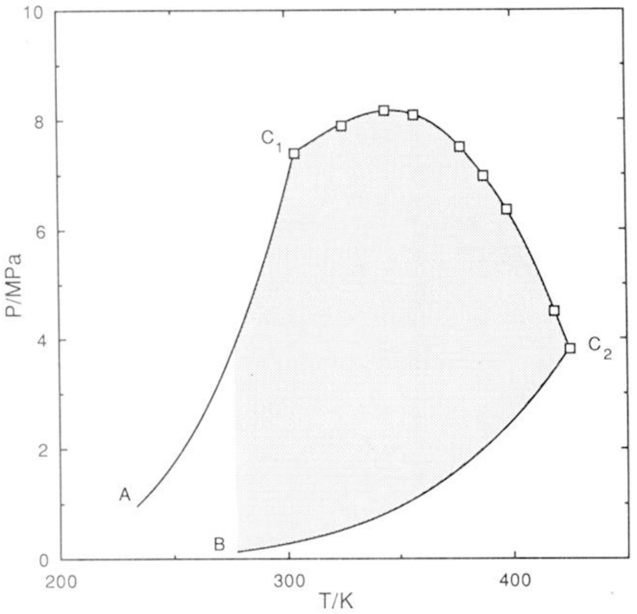

Figure 2. Pressure–temperature plot showing the vapor pressure curve of CO_2 (A–C_1), the critical line (C_1–C_2), and the vapor pressure curve of *n*-butane (B–C_2). The open squares on the critical line are points extrapolated from the data in this work. The area covered by this work is shown shaded.

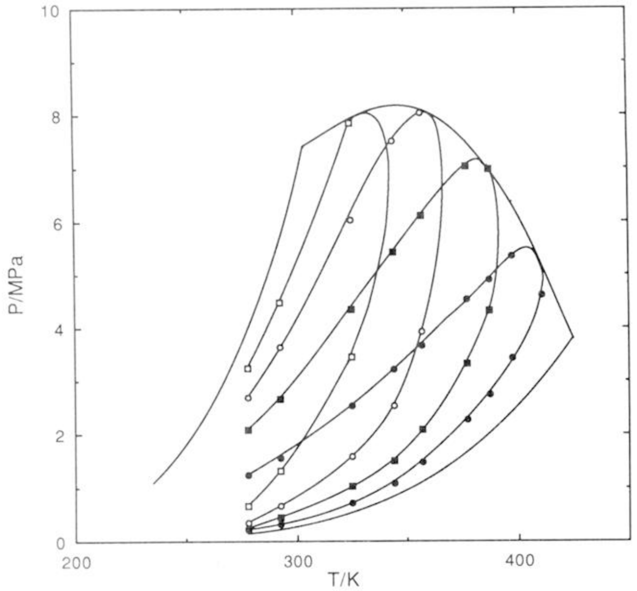

Figure 3. Pressure–temperature plot showing isopleths. ●, x_1 = 0.2; ■, x_1 = 0.4; ○, x_1 = 0.6; □, x_1 = 0.8.

The internal consistency of the data was tested by examining the consistency of simultaneous measurements of pressure, temperature, and composition by cross-plotting the data in different diagrams. Pressure–composition, temperature–composition, pressure–temperature, and *K*-value–pressure diagrams were used. Pressure–composition and pressure–temperature diagrams have already been presented in Figures 1 and 2. A pressure–temperature diagram showing curves obtained at constant composition (isopleths) was obtained from the pressure–composition diagram at four CO_2 composition

Table I. Vapor–Liquid Equilibrium Data for the Binary System CO_2 (1)/*n*-Butane (2)

P, MPa	x_1	y_1	P, MPa	x_1	y_1	P, MPa	x_1	y_1
				T = 277.90 K				
0.1246^a	0.0000	0.0000	1.0480	0.1674	0.8723	2.8062	0.6404	0.9546
0.2413		0.4450	1.3789	0.2303	0.9015	3.1095	0.7538	0.9636
0.3447	0.0390	0.6062	1.7237	0.3115	0.9202	3.4474	0.8697	0.9740
0.5171		0.7485	2.0684	0.4035	0.9338	3.6611	0.9343	0.9842
0.6826		0.8057	2.4132	0.5045	0.9444	3.9420^b	1.0000	1.0000
0.8756		0.8476						
				T = 292.60 K				
0.2042^a	0.0000	0.0000	1.2066	0.1440	0.7815	3.7576	0.6367	0.9362
0.3447	0.0191	0.2733	1.3789	0.1719	0.8155	4.2403	0.7496	0.9484
0.5171	0.0432	0.5118	1.7237	0.2275	0.8494	4.7229	0.8537	0.9616
0.6895	0.0676	0.6148	2.0684	0.2861	0.8765	5.1711	0.9329	0.9777
0.8618	0.0935	0.6995	2.5786	0.3814	0.9036	5.6532^b	1.0000	1.0000
1.0342	0.1176	0.7390	3.1371	0.4970	0.9206			
				T = 325.01 K				
0.5226^a	0.0000	0.0000	2.7717	0.2273	0.7634	6.5638	0.6620	0.8720
0.8136	0.0288	0.2622	3.1026	0.2665	0.7856	6.8947	0.7053	0.8722
1.0342	0.0506	0.3960	3.4474	0.3022	0.8034	7.2395	0.7433	0.8724
1.3927	0.0863	0.5577	3.8611	0.3497	0.8203	7.5566	0.7817	0.8687
1.7237	0.1204	0.6362	4.4885	0.4179	0.8388	7.7497	0.8063	0.8608
2.0684	0.1553	0.6956	5.2055	0.5017	0.8544	7.838^c	0.839^d	0.839^d
2.4269	0.1918	0.7325	5.8605	0.5789	0.8657			
				T = 344.25 K				
0.8323^a	0.0000	0.0000	3.1302	0.1967	0.6621	6.5431	0.5047	0.7716
1.1721	0.0295	0.2643	3.9783	0.2706	0.7141	7.2257	0.5732	0.7729
1.5789	0.0629	0.4229	4.5505	0.3227	0.7357	7.8255	0.6343	0.7700
1.7857	0.0807	0.4803	5.1711	0.3750	0.7522	8.0668	0.6674	0.7531
2.1787	0.1119	0.5612	5.8192	0.4347	0.7612	8.217^c	0.720^d	0.720^d
2.5717	0.1486	0.6074						
				T = 357.77 K				
1.1083^a	0.0000	0.0000	3.6404	0.1964	0.6028	7.0671	0.4926	0.7139
1.4824	0.0297	0.2165	4.2885	0.2503	0.6469	7.5428	0.5352	0.7116
1.9029	0.0623	0.3622	4.9573	0.3042	0.6785	7.7910	0.5647	0.6986
2.3511	0.0959	0.4577	5.6399	0.3590	0.6973	7.9289	0.5745	0.6893
2.7441	0.1283	0.5182	6.3569	0.4187	0.7107	8.070^c	0.643^d	0.643^d
3.1164	0.1567	0.5645						
				T = 377.55 K				
1.6711^a	0.0000	0.0000	4.2058	0.1877	0.4862	7.0464	0.4035	0.5664
1.9581	0.0222	0.1245	4.9918	0.2344	0.5322	7.2257	0.4318	0.5558
2.4063	0.0532	0.2477	5.5985	0.2790	0.5544	7.3912	0.4363	0.5433
3.1026	0.1014	0.3696	6.3156	0.3432	0.5692	7.443^c	0.501^d	0.501^d
3.6197	0.1382	0.4330	6.8603	0.3891	0.5699			
				T = 387.62 K				
2.0178^a	0.0000	0.0000	4.6333	0.1823	0.4213	6.4948	0.3280	0.4811
2.6269	0.0424	0.1789	5.1366	0.2175	0.4483	6.7224	0.3528	0.4750
2.9785	0.0673	0.2425	5.6123	0.2544	0.4691	6.8051	0.3590	0.4685
3.5991	0.1072	0.3283	6.2122	0.3059	0.4812	6.953^c	0.422^d	0.422^d
4.1506	0.1503	0.3858						
				T = 397.89 K				
2.4245^a	0.0000	0.0000	4.2954	0.1302	0.2994	5.8605	0.2487	0.3751
2.9234	0.0370	0.1265	4.7574	0.1619	0.3347	5.9984	0.2550	0.3732
3.4060	0.0662	0.2024	5.1366	0.1847	0.3573	6.2190	0.2773	0.3620
3.8404	0.1014	0.2524	5.5503	0.2168	0.3678	6.358^c	0.328^d	0.328^d
				T = 418.48 K				
3.4190^a	0.0000	0.0000	4.0265	0.0443	0.0804	4.3023	0.0638	0.0968
3.7714	0.0253	0.0517	4.1713	0.0546	0.0913	4.405^c	0.088^d	0.088^d
3.9093	0.0352	0.0644						

[a] Reference *11*. [b] Reference *12*. [c] Critical point on this isotherm. [d] Critical composition extrapolated from the experimental results.

values; x_1 = 0.2, 0.4, 0.6, and 0.8, and is shown as Figure 3. The values obtained are listed in Table III.

A temperature–composition diagram showing curves obtained at constant pressure (isobars) was also obtained from the pressure–composition diagram at four pressure values P = 300, 600, 900, and 1100 psia (see Figure 4). This diagram shows that the isobar curves are also smooth. The data are in Table IV.

A K-value–pressure diagram, which represents the equilibrium ratio between two phases over a pressure range, is a method widely used by the petroleum and natural gas industry. The method was first developed by Chao and Seader (*15*). The K value is defined as the equilibrium ratio between the vapor and liquid composition for each substance ($K_i = y_i/x_i$) and provides a measure of the tendency of each component to concentrate in the vapor phase. Light components have K values greater than 1, whereas the heavy ones have K values lower than unity (*16*). In Figure 5, six isotherms are plotted in a K value vs pressure diagram using logarithmic scales. There are two branches for each isotherm, one for each component.

Table II. Critical Line Values for the Binary System Carbon Dioxide (1)/*n*-Butane (2)

T, K	P, MPa	CO_2 compn ($x_1 = y_1$)	T, K	P, MPa	CO_2 compn ($x_1 = y_1$)
304.19	7.382	1.000[a]	387.62	6.953	0.422
325.01	7.838	0.839	397.89	6.358	0.328
344.25	8.217	0.720	418.48	4.405	0.088
357.17	8.070	0.643	425.16	3.796	0.000[b]
377.55	7.443	0.501			

[a] Critical point of pure carbon dioxide (*12*). [b] Critical point of pure *n*-butane (*11*).

Table III. Interpolated Values Obtained for the System CO_2/*n*-Butane along Isopleths

T, K	P_{vap}, MPa	P_{liq}, MPa	T, K	P_{vap}, MPa	P_{liq}, MPa
		$x_{CO_2} = 0.2$			
410.89	4.61		344.26	1.09	3.21
397.89	3.43	5.34	325.01	0.71	2.52
387.62	2.75	4.90	292.60	0.31	1.55
377.55	2.25	4.52	277.90	0.21	1.24
357.17	1.47	3.67			
		$x_{CO_2} = 0.4$			
387.62	4.32	6.97	325.01	1.03	4.34
377.55	3.32	7.03	292.60	0.44	2.65
357.17	2.07	6.10	277.90	0.24	2.07
344.26	1.50	5.43			
		$x_{CO_2} = 0.6$			
357.17	3.93	8.03	292.60	0.65	3.62
344.26	2.52	7.50	277.90	0.34	2.69
325.01	1.57	6.03			
		$x_{CO_2} = 0.8$			
325.01	3.45	7.83	277.90	0.65	3.23
292.60	1.31	4.48			

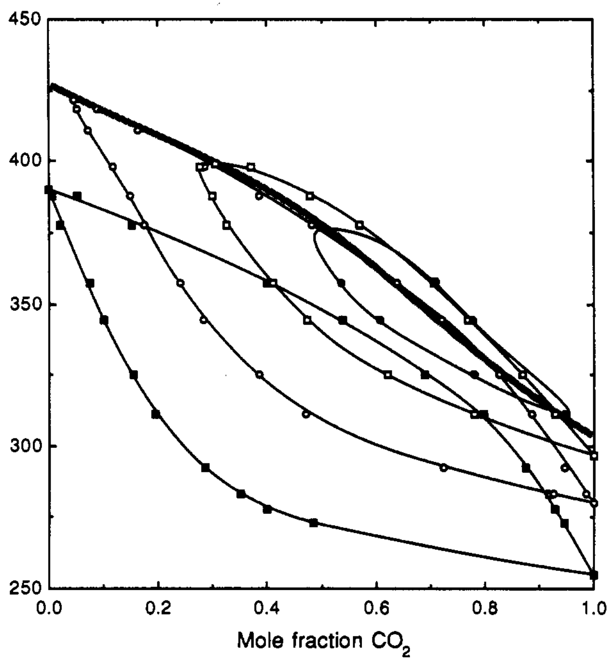

Figure 4. Temperature–mole fraction plot showing isobars. ■, P = 2.068 MPa; ○, P = 4.137 MPa; □, P = 6.205 MPa; ●, P = 7.584 MPa.

As it was expected, the CO_2 tends to concentrate in the vapor phase (K_{CO_2} value > 1) and the *n*-butane in the liquid phase $K_{n\text{-}C_4}$ value < 1). The two branches converge at the mixture critical points, where the K value = 1, and the curve exhibits a vertical tangent at that point. The degree of smoothness of the curves for each isotherm reflects the internal consistency of the data.

Table IV. Temperature–Composition Experimental Values Obtained for the System CO_2 (1)/*n*-Butane (2)

T, K	x_1	y_1	T, K	x_1	y_1
		P = 2.068 MPa (300 psia)			
387.62	0.005	0.050	310.93[a]	0.195	0.799
377.55	0.050	0.150	292.60	0.285	0.876
357.17	0.073	0.400	283.15[b]	0.350	0.916
344.25	0.100	0.535	277.90	0.400	0.930
325.01	0.155	0.691	273.15[c]	0.485	0.945
		P = 4.137 MPa (600 psia)			
418.48	0.050	0.087	344.25	0.282	0.722
410.93	0.072	0.161	325.01	0.385	0.825
397.89	0.118	0.284	310.93[a]	0.470	0.885
387.62	0.148	0.385	292.60	0.723	0.945
377.55	0.175	0.481	283.15[b]	0.925	0.987
357.17	0.238	0.638			
		P = 6.205 MPa (900 psia)			
397.89	0.275	0.369	344.25	0.473	0.770
387.62	0.300	0.480	325.01	0.620	0.869
377.55	0.326	0.569	310.93[a]	0.780	0.930
357.17	0.409	0.706		0.306[d]	
		P = 7.584 MPa (1100 psia)			
357.17	0.536	0.709		0.510[d]	
344.25	0.606	0.777			0.950[d]
325.01	0.780	0.870			

[a] Reference *5*. [b] Reference *9*. [c] Reference *8*. [d] Mixture critical point.

Table V. Data-Fitting Results Obtained Using the SRK and PR Equations of State for the System CO_2/*n*-Butane at 71.10 and 124.74 °C

EOS	T, K	k_{12}	rms(x)	rms(y)
PR	344.25	0.134	0.006 65	0.005 41
	397.89	0.181	0.004 86	0.009 25
SRK (z_{12} = 0)	344.25	0.149	0.008 13	0.006 72
	397.89	0.205	0.006 56	0.011 00

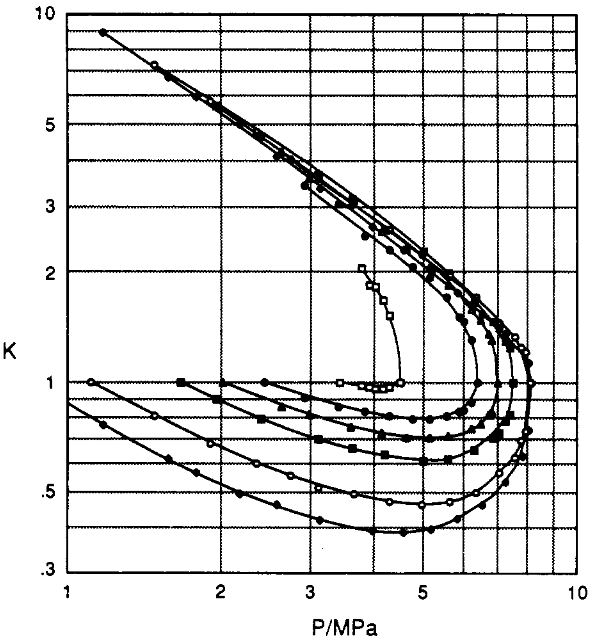

Figure 5. K-value plot versus pressure for six isotherms. ◆, T = 344.25 K; ○, T = 357.77 K; ■, 377.55 K; △, T = 387.62 K; ●, T = 397.89 K; □, 418.48 K. K_1 values are ≥1; K_2 values are ≤1.

Equations of State

The Soave–Redlich–Kwong (SRK) (*17*) and the Peng–Robinson (PR) (*18*) equations of state were fitted separately for two isotherms at 71.10 °C (344.25 K) and 124.74 °C (397.89 K). At those temperatures, CO_2 was a supercritical component,

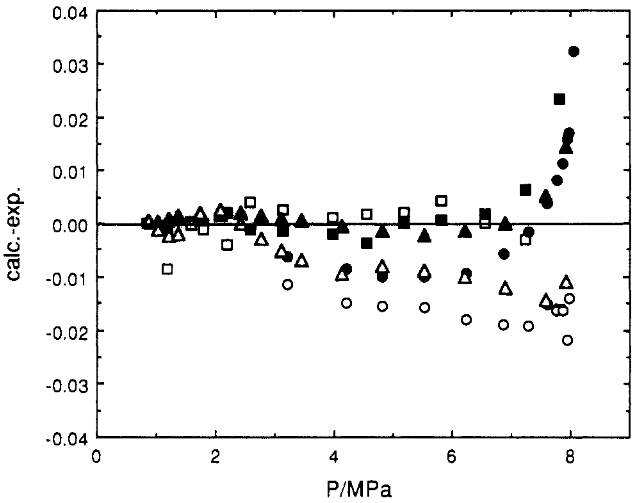

Figure 6. Deviation plot for isotherms at 344.3 K. Calculated compositions were determined from the Peng-Robinson equation using k_{ij} = 0.134. Liquid composition deviations, filled symbols; vapor composition deviations, open symbols. ■, this work; ●, ref *7*; ▲, ref *5*.

whereas the *n*-butane was subcritical. The best interaction parameters obtained for both equations, determined by minimizing the deviation of the calculated liquid composition curves from the experimental data, are displayed in Table V. At the lower temperature, the vapor-phase compositions from the PR equation were in good agreement with experiment, but the SRK compositions were too rich in CO_2. At the higher temperature, both equations of state predicted vapor compositions with too much butane.

The molar volume of the liquid mixture, as predicted by the SRK equation, was always larger than the values obtained with the PR equation. The molar volumes decreased with pressure up to a minimum, then increased until the critical point was reached. Molar volumes were not measured in this study.

Comparison with Previous Studies

The data values obtained at 71.10 °C were compared to those reported by Olds et al. (*5*) and Hsu et al. (*7*) and to calculated values at the corresponding pressures from the Peng-Robinson equation of state using the interaction parameter listed in Table V. Above 7 MPa systematic deviations (of opposite sign for liquid and vapor) show up for all the data because the calculated critical point from the PR equation at this temperature is at P = 8.06 MPa, lower than the 8.217 MPa that has been observed. Both the liquid and vapor compositions from this work are in good agreement with the PR equation below 7 MPa, but the vapor compositions of Olds et al. and both the liquid and vapor compositions of Hsu et al. are higher than the calculated values by 0.01 or more over much of the pressure range. A deviation plot showing both liquid and vapor composition deviations is given in Figure 6.

Acknowledgment

M.E.P.F. thanks the Venezuelan government for a fellowship through CEPET.

Literature Cited

(1) Cheng, H.; Pozo de Fernández, M. E.; Zollweg, J. A.; Streett, W. B. *J. Chem. Eng. Data*, preceding paper in this issue.
(2) Cheng, H.; Pozo de Fernández, M. E.; Zollweg, J. A.; Streett, W. B. Unpublished work, Cornell University, 1984.
(3) Shah, N. N.; Pozo de Fernández, M. E.; Zollweg, J. A.; Streett, W. B. Unpublished work, Cornell University, 1985; submitted for publication in *J. Chem. Eng. Data*, 1989.
(4) Shah, N. N. M.S. Thesis, Cornell University, 1985.
(5) Olds, R. H.; Reamer, H. H.; Sage, B. H.; Lacey, W. N. *Ind. Eng. Chem.* **1949**, *41*, 475.
(6) Behrens, P. K.; Sandler, S. I. *J. Chem. Eng. Data* **1983**, *28*, 52.
(7) Hsu, J. J.; Nagarajan, N.; Robinson, R. L. *J. Chem. Eng. Data* **1985**, *30*, 485.
(8) Nagahama, K.; Konishi, H.; Hoshino, D.; Hirata, M. *J. Chem. Eng. Jpn.* **1974**, *7*, 323.
(9) Kalra, H.; Krishnan, T. R.; Robinson, D. B. *J. Chem. Eng. Data* **1978**, *21*, 222.
(10) Pozo, M. E.; Streett, W. B. *J. Chem. Eng. Data* **1984**, *29*, 324.
(11) Vargaftik, N. B. *Tables of the Thermophysical Properties of Liquids and Gases*, 2nd ed.; Wiley: New York, 1975.
(12) Goodwin, R. D. *n-Butane: Provisional Thermodynamic Functions from 135 to 700 K at Pressures Up to 70 bar*; National Bureau of Standards, Thermophysical Properties Division: Boulder, CO, 1979.
(13) Schneider, G. M. *Chemical Thermodynamics*; McGlashan, Senior Reporter; Burlington House: London 1978; Vol 2, pp 105-146.
(14) Van Konynenburg, P. H.; Scott, R. L. *Philos. Trans. R. Soc. London* **1980**, *A298*, 495.
(15) Chao, K. C.; Seader, J. D. *AIChE J.* **1981**, *7*, 598.
(16) Smith, J. M.; van Ness, H. C. *Introduction to Chemical Engineering Thermodynamics*, 3rd ed.; McGraw-Hill: New York, 1975.
(17) Soave, G. *Chem. Eng. Sci.* **1972**, *27*, 1197.
(18) Peng, D.-Y.; Robinson, D. B. *Ind. Eng. Chem. Fundam.* **1976**, *15*, 59.

Received for review September 26, 1988. Accepted April 21, 1989. This work was supported by Grant CBT-8515255 from the National Science Foundation.

Liquid-Liquid Equilibria for the Hexane-Benzene-Dimethyl Sulfoxide Ternary System

George W. Cassell,[†] **Mohamed M. Hassan, and Anthony L. Hines***

Department of Chemical Engineering, University of Missouri—Columbia, Columbia, Missouri 65211

Liquid-liquid equilibrium data for the hexane-benzene-dimethyl sulfoxide system were measured at 10, 25, and 50 °C. The experimental data were correlated by using the NRTL and the UNIQUAC models.

Introduction

Liquid-liquid equilibrium data are useful for the design of liquid extraction processes. Because dimethyl sulfoxide (DMSO) is a versatile solvent for a broad range of liquids, phase equilibrium studies of the ternary mixtures of dimethyl sulfoxide has received a great deal of attention (*1-3*). The purpose of the present study was to investigate the liquid-liquid equilibria for the hexane-benzene-dimethyl sulfoxide system at 10, 25, and

---

[†] Current address: Conoco Oil Co., Ponca City, OK.
* To whom correspondence should be addressed.

0021-9568/89/1734-0328$01.50/0